Colloid and Polymer Science (2018) 296:883–893
https://doi.org/10.1007/s00396-018-4299-6

ORIGINAL CONTRIBUTION

Effect of cellulose beads on shear-thickening behavior in concentrated polymer dispersions

Ehteshamul Islam[1,2] · Gurkiran Kaur[2] · Debarati Bhattacharjee[2] · Suman Singh[3] · Ipsita Biswas[2] · Sanjeev K. Verma[2]

Received: 12 October 2017 / Revised: 19 January 2018 / Accepted: 1 March 2018 / Published online: 20 March 2018

Abstract

In the present work, we investigated the role of cellulose beads as additive for tuning of shear thickening (ST) behavior of traditional colloidal silica-based shear thickening fluids (STFs). STFs were synthesized with colloidal silica in liquid polyethylene glycol (PEG-200). The ST behavior of cellulose-based STF was compared with silica-based STF in terms of the steady-state and dynamic rheological studies while keeping the same total mass loading in PEG-200 polymer matrix. The ST behavior of cellulose-based STF was found to be more than three times higher than the silica-based STF at the same concentration. It can be expected that the cellulose beads with dense surface hydroxyl groups are a prime reason for improved interfacial interaction between the liquid PEG chains and the PEG-coated silica nanoparticles through strong hydrogen bonding. Both the steady-state and dynamic rheological analyses confirmed the better shear thickening and strain thickening behavior, respectively, as well as higher energy absorption property for cellulose-based STFs. The improved ST behavior of porous cellulose-based STF is definitely due to the cluster formation. This has been justifiably complemented by SEM and in situ rheological microscopy analyses.

Keywords Shear thickening fluid · Strain thickening · Cellulose beads · Additive · Dispersion · Rheology

Introduction

Shear thickening is one of the most interesting rheological phenomena of colloidal suspensions observed over the past decades [1]. Shear thickening is a characteristic behavior in concentrated suspension composed of hard particles which usually show an exponential increase in viscosity when the shear rate increases to a critical value [2, 3]. At low shear rates, the shear thickening fluid (STF) has low viscosity and flows easily. However, when a sudden impact is applied (at higher shear rates), the fluid is transformed into a solid-like state.

Various mechanisms have been formulated to explain shear thickening behavior of concentrated suspensions. In a very early study, Hoffman (1972) had proposed that at higher deformation rate, an order-disorder transition of particles causes rise in viscosity [4, 5]. However, the most widely accepted mechanism is the shear-induced "hydroclusters" in which hydrodynamic lubricating forces completely overcome the interparticle repulsive forces at high shear rate, and this results in shear induced self-assembled hydroclusters that increase the viscosity. This hypothesis was further supported by a detailed rheological, optic-SANS, and simulation studies [6–9].

The systematic tuning of rheological properties of STFs, to a point where its fluid-like behavior is transformed into a solid-like non-linear state, makes it a good choice for various engineering applications [10–15] such as body armors, damping devices, smart structures, and medical devices etc. Chu et al. observed that shear thickening behavior of STF is drastically effected by the surface properties of silica particles [16]. Petel et al. [17, 18] investigated the particle strength and bulk density of STF on ballistic resistance. According to their findings, increased thickening behavior and particle strength

Electronic supplementary material The online version of this article (https://doi.org/10.1007/s00396-018-4299-6) contains supplementary material, which is available to authorized users.

✉ Sanjeev K. Verma
skv002002@gmail.com

Ehteshamul Islam
ehteshamulislam@outlook.com; eislam@polymers.iitd.ac.in

[1] Department of Materials Science and Engineering, Indian Institute of Technology, Hauz Khas, New Delhi, Delhi 110016, India

[2] Terminal Ballistics Research Laboratory, DRDO, Sec 30, Chandigarh 160030, India

[3] Central Scientific Instruments Organisation, CSIR, Sec 30, Chandigarh 160030, India

under dynamic conditions are the main cause for ballistic resistance of the STFs. Impregnation of STFs on conventional ballistic materials, such as Kevlar, was observed to enhance their ballistic performance and was found advantageous as it can retain their flexibility with an overall reduction of weight of the fabric [19–24].

Hunt et al. [25] investigated the use of STF to control the stiffness of composite structures by controlling rheological properties and discussed their future applications in the fields of aeronautics, aerospace, sports equipment, and consumer goods. William et al. [26] examined STF-based medical clothing and support structures, where they exploited the viscosity change on a sudden acceleration to prevent the puncture prone area of body parts from sudden impact. Galindo-Rosales et al. [27] have developed environment-friendly composite structure made up of micro-agglomerated cork sheets engraved with micro-channel network filled with STF.

The rheological properties of silica made STFs depend upon various factors such as their shape [1], size [28], polydispersity of dispersed particles [29], polymeric matrix, and the method of STF preparation. Besides these parameters of the system itself, particle surface modification and the constitution of different additive would also affect the rheological properties of STFs.

Various attempts were carried out to control the shear thickening behavior of STFs by the addition of different additives, or by surface modification of nanoparticles [16, 30–35]. However, all the methods suffered from one or more limitations, such as low rise in viscosity or multiple step protocols for the modification of nanoparticles. Recently, the effect of spherical porous silica nanoparticles on ST effect was studied and found that the porous nature of the particle increases the ST behavior at fairly low concentration (42.5 wt%) [36].

Cellulose beads are spherical porous particles with diameters usually in the range of micron to millimeter. Spherical porous cellulose beads are a new class of cellulose materials that are characterized by high crystallinity and are used as reinforcing filler in polymers [37]. Cellulose beads offer high porosity, high mechanical strength, and unique functional properties due to sufficiently large numbers of reactive hydroxyl groups, and that makes it a great choice for the biochemists and biotechnologists. Due to the said properties, cellulose beads and their derivatives find its application in enzyme immobilization, chromatographic techniques, carriers for drug delivery, heavy metal ion removal, adsorbants, and biocatalysis etc. [38–43]. Therefore, the porous nature of cellulose beads along with the abundance of functional hydroxyl groups makes it outstandingly suitable for playing the role of a highly effective additive to control the shear thickening behavior of silica-based STF. Higher ratio of surface hydroxyl groups in cellulose beads is expected to improve the shear-thickening behavior by improving the interaction between nanoparticles and polymeric matrix. However, till date as per our best knowledge, no work has been reported in literature for the improvement of shear-thickening behavior by addition of cellulose beads as an additive.

In this study, we have varied the concentration of cellulose beads and studied the effect of spherical porous cellulose beads as an additive on the rheological behavior of monodispersed silica-based STF.

Materials and methods

Materials

Silica nanoparticles of primary particle size (600 nm supplied by Om Laboratory, India) and polyethylene glycol with molar mass of 200 g/mol (Merck, India) were used for the synthesis of shear-thickening fluids. Porous cellulose particles (supplied by Om Laboratory, India) were used as additive to tune the thickening behavior of STF. The average particle size of silica nanoparticles was measured through DLS using Brookhaven instrument (Fig. 1a), and also through SEM using Evo/MA 15 Zeiss instrument (Fig. 1b). The average particle size of silica nanoparticles was found to be 594 nm from DLS and 602 nm from SEM. The particle size and nature of cellulose particles were measured by SEM analysis using Evo/MA 15 Zeiss instrument as shown in Fig. 8a. The average particle size of cellulose beads was 89 μm.

Method of preparation of STF dispersion

In the present study, STF with 62% weight percentage was prepared by sonochemical method using ethanol as a solvent. The nanoparticles were dispersed in excess of ethanol using Cole Palmer Ultrasonicator Disperser at a frequency of 24 kHz at a frequency of 75 W/cm^2 for 10 min. After complete wetting of silica particles, polyethylene glycol (PEG-200) (liquid, 120 or 114 g) was added to the mixture and again sonicated for another five spells of 10 min. The temperature of reaction mixture was kept below 40 °C. The ethanol was evaporated at 90 °C, and reaction mixture was kept at vacuum for 6 h to remove any traces of solvent and air bubbles. The silica nanoparticles and cellulose were added in equal proportion as additives to the synthesized STF (62 wt%) to achieve different mass loading percentage of silica and cellulose STFs, respectively. The sonication procedure was thoroughly applied to all the mixtures for uniform dispersion of added silica or cellulose in the STF. The synthesized STFs with different weight percentage of silica and cellulose are presented in Table 1.

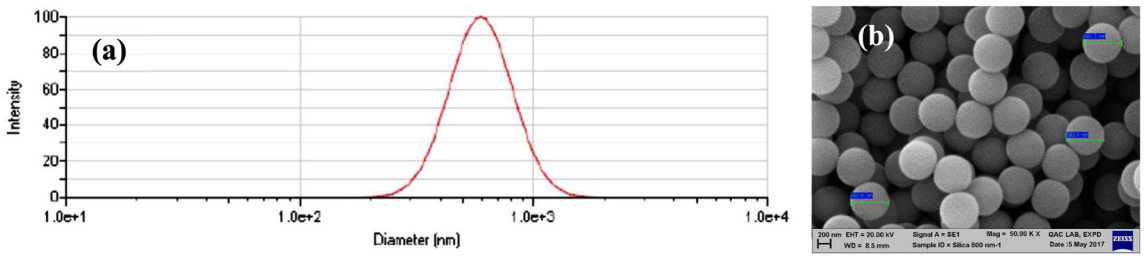

Fig. 1 **a** DLS graph and **b** SEM micrograph of silica nanoparticles used in the synthesis of STF (Avg. particle size 594 nm and PDI = 0.1)

Rheological characterization

Both steady and oscillatory shear tests (i.e., amplitude sweep test and frequency sweep test) for all the prepared STFs (Table 1) were carried out by Physica MCR 52, Anton Paar, Germany. The cone-plate geometry with a cone angle of 1° and 40 mm plate diameter at a gap of 0.08 mm was selected for the test. Steady shear measurements were conducted to observe the change in viscosity and stress values of STF with increasing shear rate. While in the oscillatory tests, both the strain sweep at constant frequency and the frequency sweep at constant strain were carried out to understand the viscoelastic response of the shear-thickening fluids. In order to remove the effects of previous shear history, all samples were pre-sheared at a shear rate of 1 s^{-1} for 120 s and then relaxed for 180 s before the test. All the silica/cellulose/PEG STF measurements were carried out at 25 °C.

Rheological microscopy test was conducted on Physica MCR-702 Twin Drive rheometer from Anton-Paar, Germany. In rheo-microscopy test, a microscope is connected to the rheometer which recorded the real-time in situ structural change under deformation. A 45-mm diameter transparent glass plate was used for the study. Microscopy test was carried out under oscillatory shear mode.

Results and discussion

The simplest way to alter shear-thickening (ST) behavior is simply tuning the concentration or mass fraction of silica nanoparticles in polymeric matrix (PEG). STFs with different silica mass fractions were achieved by addition of extra silica nanoparticles in synthesized STF-62 wt% (Table 1).

Steady-shear rheological analysis

Figure 2 shows the variations of added silica nanoparticles and cellulose beads in comparison of the steady shear response of the synthesized STFs to their corresponding ST behavior. It was observed from Fig. 2a that with increasing mass fraction of silica nanoparticles, a sudden rise in the maximum viscosity (η_m) of the STF was observed. The η_m value increased from 60 to 224 Pa.s as the mass loading of silica was increased to 63.98 wt%. No further addition of silica nanoparticles above 5.2 wt% (STF-62% + S-5.2%) was possible because the saturation limit was reached. Therefore, 224 Pa.s is the maximum value of viscosity that can be achieved by conventional method of tuning silica content in STF. The rise in viscosity can be attributed to increase in inter-particle forces with the increase in concentration of silica nanoparticles as additive.

In order to study the effect of cellulose beads on shear-thickening behavior of STF, cellulose beads were added in equivalent mass fraction, similar to the tuning of STF with the silica nanoparticles in STF-62% (Table 1).

The steady-shear rheology of the cellulose-based STFs was carried out, and results were compared with only-silica-based systems. It was observed as shown in Fig. 2b that the viscosity increases continuously with the increase in concentration of cellulose beads, as was previously observed with the addition of silica nanoparticles in the base STF (62%).

However, the rise in viscosity was 3.7 times higher and reached to a η_m value of 848 Pa.s (STF-62% + C 5.2%) as compared to only-silica-based system (STF-62% + S 5.2%) which is shown in Table 2. The rheological parameters of steady shear analysis are presented in Table 2.

Table 1 Mass percentage specification of cellulose-added STF-62%

STF	STF 62% (g)	Added silica (S)/cellulose beads (C) (g)	Added silica (S)/ cellulose beads (C) loading in STF (%)	Total mass loading[a] (%)
STF-62%	10	0	0	62
STF-62% + A-2%	9.80	0.20	2.0	62.80
STF-62% + A-3%	9.70	0.30	3.0	63.10
STF-62% + A-4%	9.60	0.40	4.0	63.50
STF-62% + A-5%	9.50	0.50	5.0	63.90
STF-62% + A-5.1%	9.49	0.51	5.1	63.94
STF-62% + A-5.2%	9.48	0.52	5.2	63.98

A additive, *C* cellulose as additive, *S* silica as additives

[a] Total silica loading (silica as additive), silica + cellulose loading (cellulose as additive)

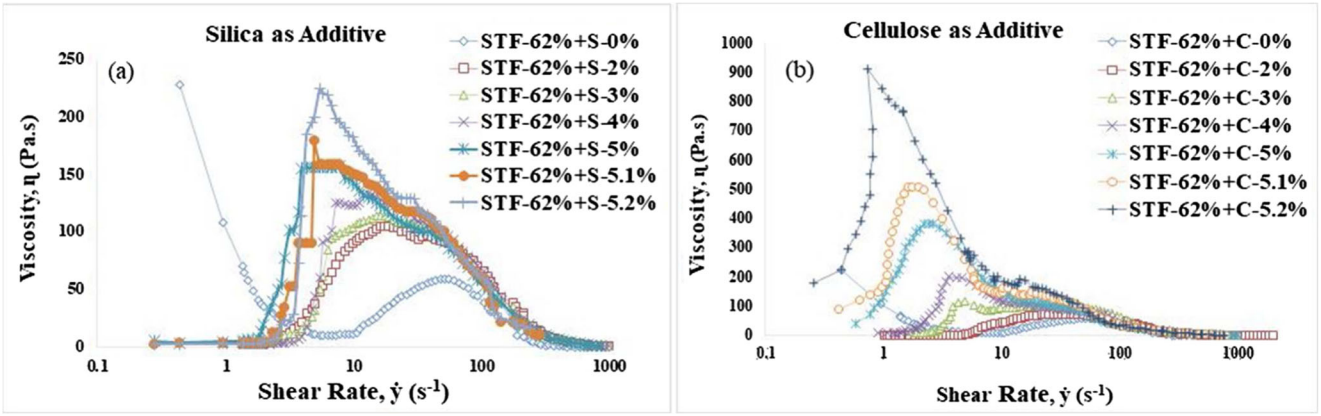

Fig. 2 Steady-state viscosity as a function of shear rate for STF at different particle loadings of (**a**) silica (where 'S' was designated in nomenclature for silica additive) and **(b)** cellulose beads (where 'C' was designated in nomenclature for cellulose additive) in PEG-200

Previous studies revealed that the suspensions at higher particle concentrations influence the flow behavior of their neighboring particles due to enhanced inter-particle interactions [44]. As a result, the viscosity becomes shear sensitive, and a sharp rise in the viscosity profile usually occurs [1, 45–48]. It has been found that the viscosity profile increases as the concentration of additives increases [35, 49–51]. We have found a similar trend in the viscosity profile as the concentration of silica and cellulose particles increases in the base STF. It is clearly evident from Fig. 3a that cellulose particles used as additive have shown a significant increase in the viscosity profile compared to that of silica-based STFs.

In Fig. 3b, effect of additive concentration on critical shear rate is shown. It is widely reported that with the increase in silica loading in the suspension, the critical shear rate decreases and leads to an increase in the viscosity of the system [52–54]. Gürgen et al. [55] have shown the effect of ceramic particles, as an additive, on ST effect of STF. In their study, the particles of SiC, Al_2O_3, and B_4C at 5 wt% loading have not shown any significant ST effect as compared to silica-based STF. Furthermore, increasing the concentration of ceramic additives leads to an increase in critical shear rate and simultaneously showing shear thinning. Usually, at higher loading of particles, the flow of polymeric liquid (PEG-200) gets restricted due to increase in effective particle loading, which is usually a condition of hydrocluster formation. In our study, it was found that the cellulose particles have shown a weaker inter-particle repulsion at higher concentration (STF 62–5.1% and STF 62–5.2%) due to their higher surface hydroxyl density and can easily be overcome by hydrodynamic lubrication forces at a lower shear rate. With the help of simulation, Brady and Bossis [6] proved that the ordering of particles is not possible in a system with weak inter-particle repulsion. Therefore, in both silica- and cellulose-based STFs, critical shear rate was found to be reduced as the additive loading increased. However, at 5% loading of silica additive, the STFs reached the maximum critical loading, which makes its critical shear rate to reach an equilibrium plateau and remain constant. On the other hand, the

Table 2 Comparison of rheological parameters between cellulose and silica nanoparticles

Rheological parameters	STF 62% + A-0%	STF 62% + A-2%	STF 62% + A-3%	STF 62% + A-4%	STF 62% + A-5%	STF62% + A-5.1%	STF62% + A-5.2%
Critical viscosity (S)	10.9	2.99	2.87	2.72	4.22	2.93	2.68
Critical viscosity (C)	–	1.6	9.6	11.5	115	89.7	182
Maximum viscosity (S)	59.4	105	114	133	157	159	224
Maximum viscosity (C)	–	75.9	115	203	385	509	848
Critical shear rate (S)	7.32	1.98	1.63	1.51	1.37	1.4	1.37
Critical shear rate (C)	–	1.98	1.7	1.37	0.956	0.434	0.227
Shear rate at Max. viscosity (S)	52	18.9	15.2	13.1	9.29	7.32	6.74
Shear rate at Max. viscosity (C)	–	27.8	4.3	3.58	2.18	1.74	0.956

A additive, *C* cellulose as additive, *S* silica as additives

Viscosity in Pa.s, shear rate in s^{-1}

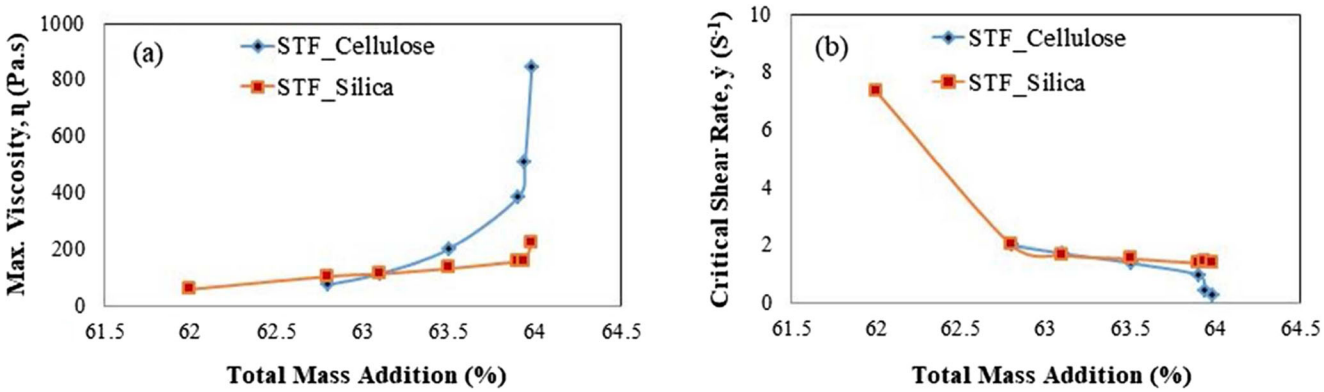

Fig. 3 (**a**) Viscosity profile and (**b**) critical shear rate of the STFs with different concentration of silica and cellulose additives

cellulose-based STFs have shown a constant decrease in the critical shear rate with increasing loading. At a very low concentration (5 wt%) of cellulose, weak inter-particle repulsion at lower critical shear rate does not support the possibility of any ordering of particles; thus, cluster growth could be the only reason for the rise in viscosity. As a consequence, viscosity profile increases significantly which can be seen by the steep increase in maximum viscosity in Fig. 3a. Therefore, from steady shear tests, it can be concluded that cellulose-based STFs have a better ST property as compared to the silica-based systems.

Dynamic rheological analysis

The oscillatory tests are the essential tools for understanding the viscoelastic response of the shear-thickening fluids. The changes in the dynamic modulus parameters, such as elastic modulus (G′), loss modulus (G″), complex modulus (G*), and complex viscosity (η*), provide the microstructure details existing in the system [56]. Oscillatory tests therefore give a more direct correlation with microstructure than steady-shear rheology [57]. In the present work, oscillatory tests (i.e., amplitude sweep

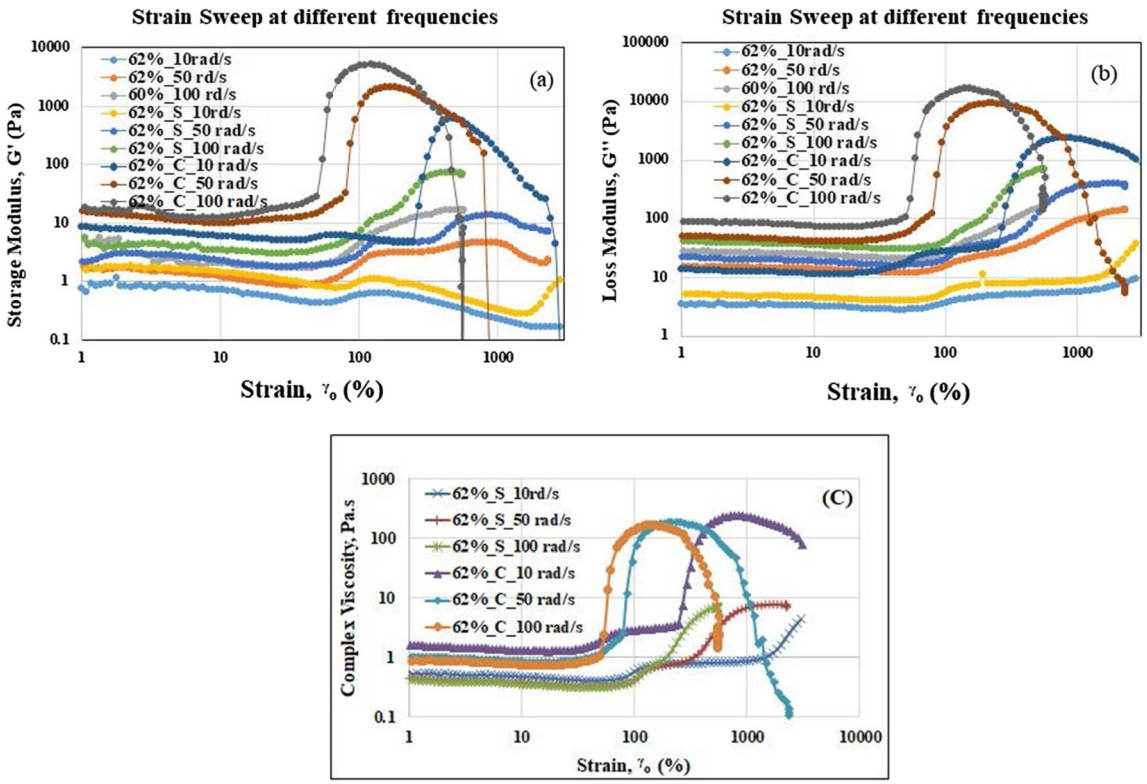

Fig. 4 Change in the **(a)** storage modulus and **(b)** viscous modulus as a function of strain amplitude at different frequencies viz., 10, 50, and 100 rad s^{-1} in STF 62% + S-5.2% and STF 62% + C-5.2%. (**c**) Complex viscosity response of STF 62% + S-5.2% and STF 62% + C-5.2% as a function of %strain at 10, 50, and 100 rad/s frequencies, respectively

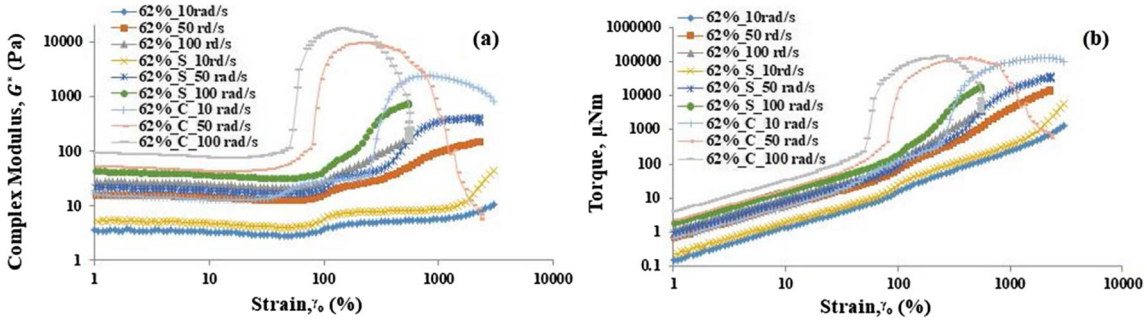

Fig. 5 Strain amplitude sweep data of silica-based and cellulose-based STFs (STF 62% + S-5.2% and STF 62% + C-5.2%) at different frequencies, **(a)** complex shear modulus vs %strain and **(b)** Torque vs %strain

test and frequency sweep test) were performed on STF-62%, STF-62% + S-5.2%, and STF-62% + C-5.2%.

Amplitude sweep tests

In amplitude sweep test, the strain sweeps obtained at different frequencies were expressed as a function of the complex shear modulus$|G^*|$. It is a measure of the material's overall resistance to deformation.

Complex modulus is a function of both storage and loss modulus and is expressed as follows:

$$G^* = G' + iG''$$

The complex viscosity is the ratio of the dynamic modulus to the frequency of deformation, represented as follows:

$$\eta^* = \frac{G^*}{\omega}$$

Amplitude sweep tests were performed at constant frequencies of 10, 50, and 100 rad/s between the strain limit from 1 to 3000% and their viscoelastic responses, such as storage modulus, loss modulus, complex modulus, and torque, and they are shown in Figs. 4 and 5. In Fig. 4a, and b, initially at lower strain, G′ and G″ are declining with increasing strain amplitude. In all the three compositions, after a critical strain limit, both modulus moieties show an abrupt increase in their values, and this shows their strain-thickening behavior [53]. In the case of cellulose-based STF (62% + C-5.2%), with increasing frequency, the jump in the modulus is significantly higher (more than 10 times) than silica-based STF (62% + C-5.2%). Moreover, loss modulus (G″) is invariably higher than the storage modulus (G′) values which is the characteristic of a non-flocculated dispersion system. Similar study was reported by Laun et al. [11], where with increasing strain, the concentrated dispersion has shown a sudden jump in viscosity by a factor of hundred and makes the dispersion highly viscous. In this study, in all compositions, the critical strain required for the onset of strain-thickening was found to be decreasing with increasing frequency.

Thus, at very high frequency (100 rad/s), the rise in complex viscosity was more rapid as compared to the lower frequencies. This sudden jump in η* may be attributed to (i) the formation of hydrogen bonds reduces the interparticle distance between the PEG-coated silica particles and (ii) the rapid increase of hydrodynamic forces increases the probability of hydrocluster formation with increasing frequency. Moreover, from complex viscosity results (Fig. 4c), it was observed that the critical strain for strain-thickening in cellulose-based STF (STF 62% + C-5.2%) was found to be independent of frequency at higher frequency of 50 and 100 rad/s (shown in Table 3), verifying the condition for strain thickening [58].

Complex shear modulus and torque response of the STF are being represented in Fig. 5. The complex shear modulus increases with the increase in deformation frequency, showing the resistance of STFs to deformation. Raghvan et al. [58] termed this phenomena as strain-thickening behavior, which was corroborated with the rise in complex modulus values, appeared at lower strain amplitude as the frequency of deformation increases. The complex shear modulus response was

Table 3 Critical strain and critical frequencies for strain thickening

STF nomenclature	Silica loading in STF (%)	Cellulose bbead loading in STF (%)	Critical strain (γc, %) for strain thickening			Critical frequency for strain thickening (ω_c, rad/s)	
			10 (rad/s)	50 (rad/s)	100 (rad/s)	250% (Strain)	500% (Strain)
STF 62%	62	–	44.8	38.3	35.4	28.5	13.2
STF 62% + S-5.2%	62% + 5.2%	–	48.6	41.5	38.4	21.5	12.3
STF 62% + C-5.2%	–	62% + 5.2%	17	14.6	14.3	3.76	3.5

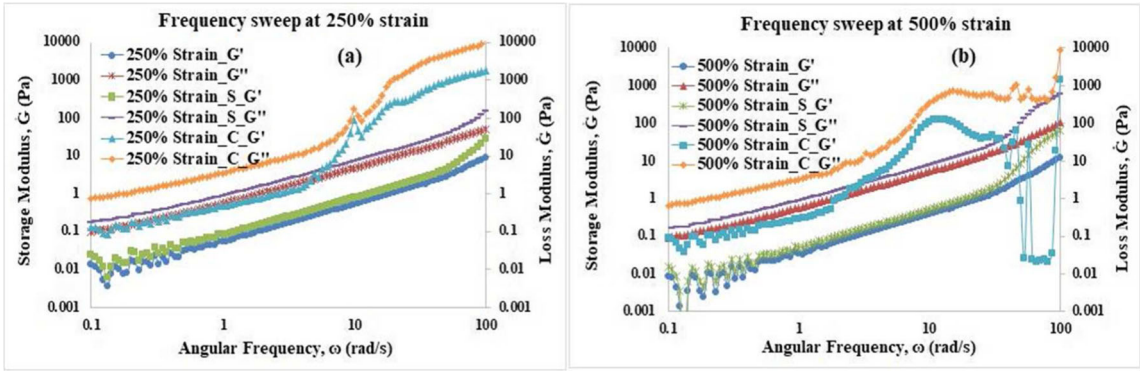

Fig. 6 Frequency sweep for base STF and STFs with highest achieved loading (STF 62% + 5.2%) of silica and cellulose at **(a)** 250% and **(b)** 500% strain amplitudes

adequately complemented by the rise of torque in STF 62% + S-5.2% and STF 62% + C-5.2% in Fig. 5b. Lee et al. [19] demonstrated that the force required in yarn pullout test of Kevlar fabric impregnated with STF was increased. This increase in yarn pullout force was correlated with the higher energy dissipation in pulling out a single yarn from the STF-coated fabric as compared to the uncoated fabric. In this study, it was found that the STF with highest concentration of cellulose loading have shown a 10 times higher torque with increasing frequency as compared to the silica-based STF. Therefore, STF (STF 62% + C-5.2%) with cellulose beads was by far most resistant to the increasing deformation frequencies and therefore showing significantly higher strain-thickening effect. We can therefore assume that the cellulose-based STF has the potential to be used in textile coating for high impact energy absorption.

Frequency sweep tests

The frequency sweep tests were conducted at constant strain amplitudes of 250 and 500% (Figs. 6 and 7) with variable frequencies. Figure 6a, b shows the storage modulus and loss modulus response with frequency on STFs at 250 and 500% strain, respectively. From Fig. 6a, and b, it is evident that, in case of STF with cellulose beads (STF 62% + C-5.2%), the moduli at a critical frequency increase abruptly with the increase in strain amplitude from 250 to 500%.

This increase in the resistance to deformation with higher strain amplitude may be attributed to the increased hydrogen bonding between the cellulose beads and silica-PEG surfaces, which consequently contributing to the increase in moduli. Similarly, in Fig. 7 (plot of complex viscosity vs. angular frequency), a rise in complex viscosity with increasing strain amplitude was observed. The STF with cellulose beads has shown a steep rise in complex viscosity at a higher strain of 500%. In comparison with complex viscosity at 500% strain, the viscosity at 250% strain did not show a steep rise rather it was a gradual rise. It is also evident from Fig. 7 that as the strain increases, the cellulose-based STF shows a lower critical frequency for the rise in complex viscosity, as compared to the silica-based STF (Table 3). This sets a typical example of strain-thickening phenomenon [58].

It is evident from both the frequency sweep and the strain sweep experiments that cellulose-based STF is highly resistant to deformation as their critical strains or critical frequencies at

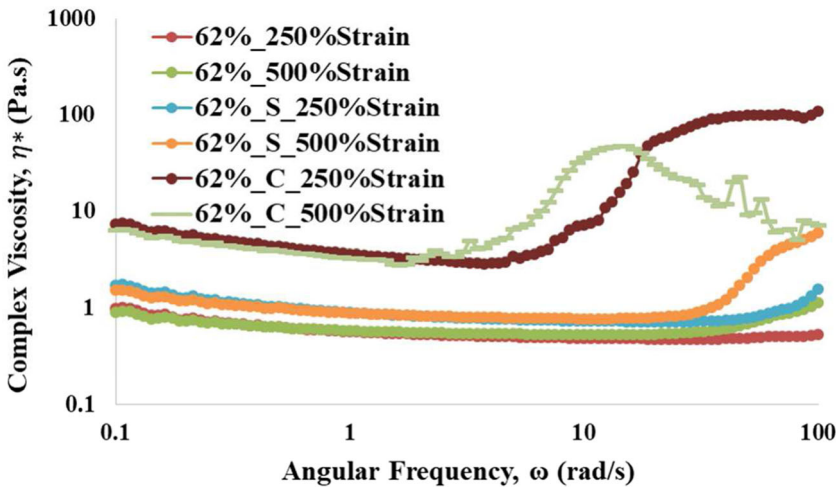

Fig. 7 Change in the complex viscosity as a function of angular frequency at 250 and 500% strain amplitude

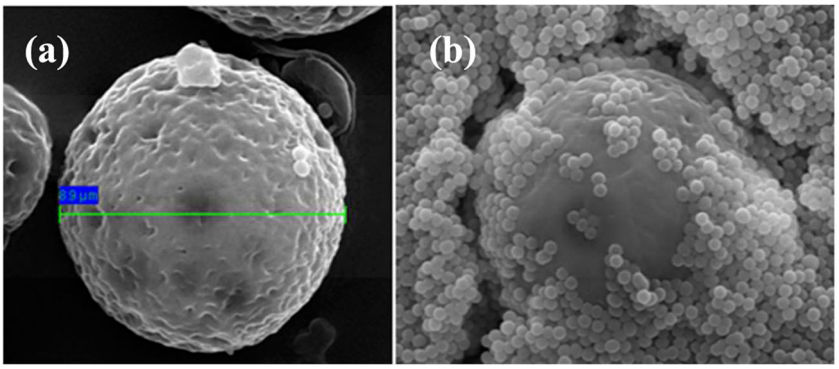

Fig. 8 **a** Porous cellulose beads (Avg. particle size 89 μm) and **b** cellulose beads in STF

higher frequencies (50 and 100 rad/s) or at higher strains (250 and 500%) remain constant (Table 3). Based on the rheological results, it can be assumed that the improved strain-thickening behavior with cellulose beads most probably due to the higher hydroxyl group density and also due to their porous nature (Fig. 8a).

Justification for hydrocluster formation

The consensus on ST effect in concentrated dispersions has been attributed to the fact that, at higher shear rate, the inter-particle distance reduces due to increase in the hydrodynamic lubrication force, and this diminished distance leads to displacement of the dispersing liquid between the silica particles [59]. The addition of micron size porous cellulose beads in the base STF (62 wt%) due to their polar nature should positively bring about a closer interaction with the PEG molecules. It has been widely reported that hydroxyl group on cellulose favors strong inter-molecular hydrogen bonding with etheric oxygen present on the PEG backbone [60–63]. Kondo et al. have studied the hydrogen bonding in regioselectively methyl substituted cellulose and PEO/PVA blend system. They revealed that the primary hydroxyl group at C-6 of cellulose has shown strong inter-molecular hydrogen bonding with ether oxygen in the PEO [62]. Moreover, the hydrophilic

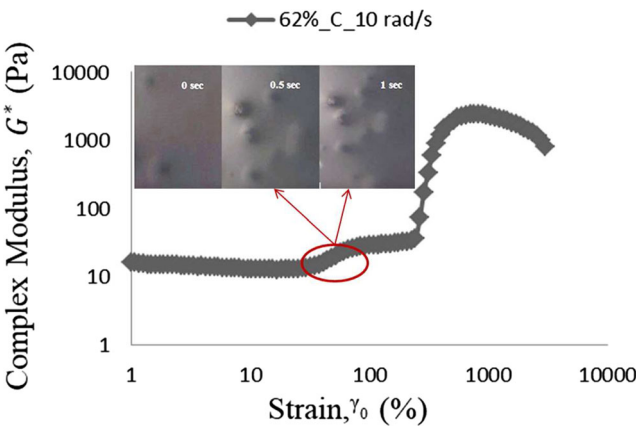

Fig. 9 Rheological microscopy of STF (62% + C-5.2%)

cellulose beads with the abundance of surface hydroxyl groups bind the remaining PEG molecules on to their active sites through hydrogen bonding and thereby improving the interaction between the PEG molecules and the PEG-coated silica particles (Fig. 8). Raghvan et al. (2000) proposed that hydrogen bonding between silanol group on silica surface with oligomeric liquids forms a denser solvation layer, which leads to an increase in short range repulsive forces and thus stabilizes the sol [30]. Chu et al. concluded that thicker solvation layer exhibits stronger repulsive force, which results in a pronounced ST effect [16]. We can therefore assume that in our study, the porous cellulose with more hydroxyl groups can increase the thickness of the solvation layer through more numbers of hydrogen bonds with PEG and PEG-coated silica surfaces. However, the PEG is a low molecular weight polymer and is supposed to exhibit a weak steric effect with the cellulose beads. Therefore, with an increase in shear or strain, formation of hydroclusters takes place at lower shear or strain value (Fig. 8b).

Hydrocluster formation was further observed in rheological microscopy study (given in Fig. 9). The optical system was mounted on the optical frame and positioned in sideway to focus the sample gap between the two plates. The combination of counter rotating plates with adjustable optical system creates a stagnant frame to capture the real-time image of sample under deformation. In rheo-microscopy study, strain sweep experiment was conducted at 10 rad/s to confirm the cluster formation. Figure 9 displays the microscopy result of STF containing porous cellulose beads. During the experiment, initially the cellulose beads were observed scattered. However, as the strain increased, these beads came closer to each other at a lower strain, showing the cluster formation. It may therefore be concluded that the strain-thickening phenomenon observed in the cellulose-based STF systems can be attributed to the (i) dense surface hydroxyl groups and (ii) porous surface architecture of cellulose beads and thus both the factors have contributed to improving the interaction with the PEG-coated silica nanoparticles.

The rise in viscosity in silicone oil-based STF with higher hydroxyl group was also observed by Zhang et al. 2014 [64]. Surface coating of particles with hydroxyl terminated

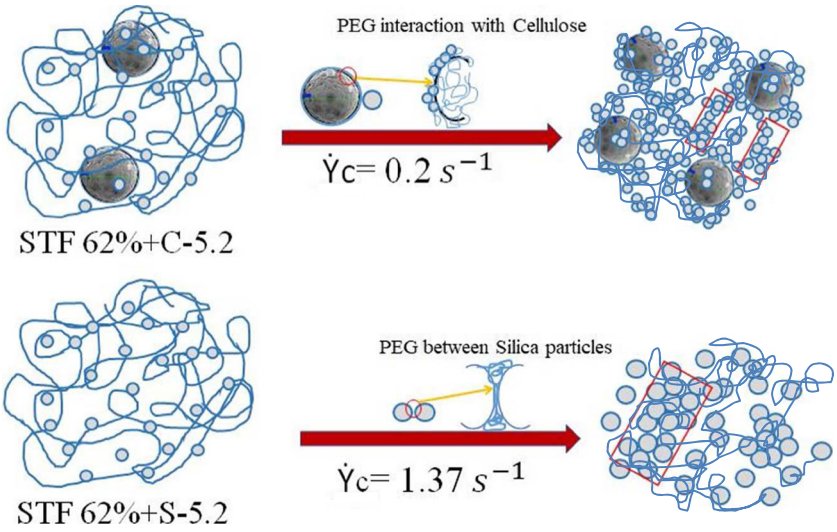

Fig. 10 Possible mechanism for shear thickening in porous cellulose-based STF

surfactants has also shown higher increase in particle agglomeration through hydrogen bonding, resulting in the improvement of ST [65].

Proposed mechanism for shear thickening

A possible mechanism for ST behavior in cellulose- and silica-based STF is explained in Fig. 10. An ideal situation is supposed to prevail where the remaining PEG molecules in the prepared STF will preferentially interact with the added porous cellulose beads through hydrogen bonding. The cellulose additive might act as a bridge between the silica-coated PEG and the remaining PEG molecules to strengthen further the interaction between the silica nanoparticles and the remaining PEG molecules. Moreover, Raghavan et al. [58] and Bossis et al. [6] suggested that elongated clusters contribute much more to the thickening behavior than the spherical ones. Gürgen et al. [55] argued that higher concentration of additive particles can be considered as barriers for elongated hydrocluster formation. However, in this study, a very low concentration of cellulose was used as an additive which does not significantly reduce the silica concentration in the final STF, and therefore, silica is still the main constituent of the STF. Further, the formation of hydroclusters, having no resistance from cellulose particles, goes unhindered because at such a low concentration, these cellulose beads would rather allow the formation of contact network between silica nanoparticles along with a strongly hydrogen-bonded cellulose-PEG assembly.

Conclusion

In this study, it was demonstrated that the application of cellulose beads as a novel additive for enhancing the shear-thickening behavior of conventional silica-based STF. Porous cellulose-based STF showed a 3.7 times rise in the shear viscosity as compared to only-silica-based STF at the same mass loading. As compared to non-porous silica nanoparticles, porous cellulose beads with higher hydroxyl group density showed significantly better interaction with the PEG and PEG-coated silica in the STF. This is further confirmed by SEM and rheo-microscopic analyses. The dynamic rheology of cellulose-based STF further confirms the higher strain-thickening behavior and higher energy absorption and this was reflected by their sudden rise in complex viscosity, storage modulus, loss modulus, and torque values as compared to the rheological properties of conventional silica-based STFs. At higher frequencies, the onset of strain thickening at critical strain amplitude was found to be independent of frequency. Findings of this study strongly suggest that the cellulose beads can be advantageous for its application as an additive to control the onset of ST. Porous cellulose can find its application in the area where higher viscosity rise happens to be critical such as high energy absorbing ballistic suits, helmets, space suits, and shock absorbers etc. However, further studies are required to generate more conclusive results to sharpen our understanding about the working mechanism of cellulose as an additive on the ST behavior in different particle-based STF systems other than the silica-based systems.

Acknowledgments Our grateful acknowledgments are due to the Director (TBRL Chandigarh) for his kind support and encouragement. We would also like to record our gratitude to Ms. Vandana P. Arya and Ms. Gurvinder Kaur of TBRL at Chandigarh, to the Centre for Polymer Science and Engineering, Indian Institute of Technology Delhi, New Delhi and to Dr. Rajeev Mehta of Thapar University, Patiala for allowing us to use their facilities for the experimentations on the synthesis and characterization of STF.

Funding information This research work was wholly funded and supported by Terminal Ballistics Research Laboratory, Chandigarh which is a part of D.R.D.O., under Ministry of Defence, Government of India.

Compliance with ethical standards

Conflict of interest The authors declare that they have no conflict of interest.

References

1. Barnes HA (1989) Shear-thickening ("Dilatancy") in suspensions of nonaggregating solid particles dispersed in Newtonian liquids. J Rheol (N Y N Y) 33:329–366. https://doi.org/10.1122/1.550017
2. Bender J, Wagner NJ (1996) Reversible shear thickening in monodisperse and bidisperse colloidal dispersions. J Rheol (N Y N Y) 40:899–916. https://doi.org/10.1122/1.550767
3. Brady J, Bossis G (1985) The rheology of concentrated suspensions of spheres in simple shear flow by numerical simulation. J Fluid Mech 155:105
4. Hoffman RL (1972) Discontinuous and dilatant viscosity behavior in concentrated suspensions. I. Observation of a flow instability. Trans Soc Rheol 161:155–173
5. Catherall AA, Melrose JR, Ball RC (2000) Shear thickening and order–disorder effects in concentrated colloids at high shear rates. J Rheol (N Y N Y) 44:1–25. https://doi.org/10.1122/1.551072
6. Bossis G, Brady JF (1989) The rheology of Brownian suspensions. J Chem Phys 91:1866–1874. https://doi.org/10.1063/1.457091
7. Bender JW, Wagner NJ (1995) Optical measurement of the contributions of colloidal forces to the rheology of concentrated suspensions. J Colloid Interface Sci 172:171–184. https://doi.org/10.1006/jcis.1995.1240
8. Farr RS, Melrose JR, Ball RC (1997) Kinetic theory of jamming in hard-sphere startup flows. Phys Rev E 55:7203–7211. https://doi.org/10.1103/PhysRevE.55.7203
9. Maranzano BJ, Wagner NJ (2002) Flow-small angle neutron scattering measurements of colloidal dispersion microstructure evolution through the shear thickening transition. J Chem Phys. https://doi.org/10.1063/1.1519253
10. Helber R, Doncker F, Bung R (1990) Vibration attenuation by passive stiffness switching mounts. J Sound Vib 138:47–57. https://doi.org/10.1016/0022-460X(90)90703-3
11. Laun HM (1991) Rheology of extremely shear thickening polymer (dispersionsa) (passively viscosity switching fluids). J Rheol (N Y N Y) 35:999–1034. https://doi.org/10.1122/1.550257
12. Fischer C, Braun SA, Bourban P-E et al (2006) Dynamic properties of sandwich structures with integrated shear-thickening fluids. Smart Mater Struct 15:1467–1475. https://doi.org/10.1088/0964-1726/15/5/036
13. Zhang XZ, Li WH, Gong XL (2008) The rheology of shear thickening fluid (STF) and the dynamic performance of an STF-filled damper. Smart Mater Struct 17:35027. https://doi.org/10.1088/0964-1726/17/3/035027
14. Jiang W, Gong X, Xuan S, Jiang W, Ye F, Li X, Liu T (2013) Stress pulse attenuation in shear thickening fluid. Appl Phys Lett 102:101901. https://doi.org/10.1063/1.4795303
15. Afeshejani SHA, Sabet SAR, Zeynali ME, Atai M (2014) Energy absorption in a shear-thickening fluid. J Mater Eng Perform 23:4289–4297. https://doi.org/10.1007/s11665-014-1217-z
16. Chu B, Brady AT, Mannhalter BD, Salem DR (2014) Effect of silica particle surface chemistry on the shear thickening behaviour of concentrated colloidal suspensions. J Phys D Appl Phys 47:1–7. https://doi.org/10.1088/0022-3727/47/33/335302
17. Petel OE, Ouellet S, Loiseau J, Marr BJ, Frost DL, Higgins AJ (2013) The effect of particle strength on the ballistic resistance of shear thickening fluids. Appl Phys Lett 102:064103. https://doi.org/10.1063/1.4791785
18. Petel OE, Ouellet S, Loiseau J, Frost DL, Higgins AJ (2015) A comparison of the ballistic performance of shear thickening fluids based on particle strength and volume fraction. Int J Impact Eng 85:83–96. https://doi.org/10.1016/j.ijimpeng.2015.06.004
19. Lee YS, Wetzel ED, Wagner NJ (2003) The ballistic impact characteristics of Kevlar?? Woven fabrics impregnated with a colloidal shear thickening fluid. J Mater Sci 38:2825–2833. https://doi.org/10.1023/A:1024424200221
20. Egres Jr RG, Decker MJ, Halbach CJ, Lee YS, Kirkwood JE, Kirkwood KM, Wagner NJ, Wetzel ED (2006) Stab resistance of shear thickening fluid (STF)–Kevlar composites for body armor applications. Transformational Science and Technology for the Current and Future Force. https://doi.org/10.1142/9789812772572_0034
21. Decker MJ, Halbach CJ, Nam CH, Wagner NJ, Wetzel ED (2007) Stab resistance of shear thickening fluid (STF)-treated fabrics. Compos Sci Technol 67:565–578. https://doi.org/10.1016/j.compscitech.2006.08.007
22. Rosen BA, Laufer CN, Kalman DP et al (2007) Multi-threat performance of kaolin-based shear thickening fluid (STF)-treated fabrics. Proc. SAMPE (Baltimore, MD, 3–7 June)
23. Hassan TA, Rangari VK, Jeelani S (2010) Synthesis, processing and characterization of shear thickening fluid (STF) impregnated fabric composites. Mater Sci Eng A 527:2892–2899. https://doi.org/10.1016/j.msea.2010.01.018
24. Majumdar A, Butola BS, Srivastava A (2014) Development of soft composite materials with improved impact resistance using Kevlar fabric and nano-silica based shear thickening fluid. Mater Des 54:295–300. https://doi.org/10.1016/j.matdes.2013.07.086
25. Hunt W III, Phelps C (1991) Method to reduce movement of a CPF device via a shear-thickening fluid. US Pat 4,982,792
26. Williams T, Day J, Pickard S (2007) Surgical and medical garments and materials incorporating shear thickening fluids. US Pat. App. 12/440,086
27. Galindo-Rosales FJ, Martínez-Aranda S, Campo-Deaño L (2015) CorkSTFμfluidics – a novel concept for the development of eco-friendly light-weight energy absorbing composites. Mater Des 82:326–334. https://doi.org/10.1016/j.matdes.2014.12.025
28. Bettin G (2007) High-rate deformation behavior and applications of fluid filled reticulated foams. Massachusetts Institute of Technology
29. Genovese DB (2012) Shear rheology of hard-sphere, dispersed, and aggregated suspensions, and filler-matrix composites. Adv Colloid Interf Sci 171:1–16. https://doi.org/10.1016/j.cis.2011.12.005
30. Raghavan SR, Walls HJ, Khan SA (2000) Rheology of silica dispersions in organic liquids: new evidence for solvation forces dictated by hydrogen bonding. Langmuir 16:7920–7930. https://doi.org/10.1021/la991548q
31. Osman MA, Atallah A (2006) Interfacial adhesion and composite viscoelasticity. Macromol Rapid Commun 27:1380–1385. https://doi.org/10.1002/marc.200600294
32. Xu Y-L, Gong X-L, Peng C, Sun YQ, Jiang WQ, Zhang Z (2010) Shear thickening fluids based on additives with different concentrations and molecular chain lengths. Chin J Chem Phys 23:342–346. https://doi.org/10.1088/1674-0068/23/03/342-346
33. Yu K, Cao H, Qian K et al (2012) Shear thickening behavior of modified silica nanoparticles in polyethylene glycol. J Nanopart Res 14:747. https://doi.org/10.1007/s11051-012-0747-2
34. Sha X, Yu K, Cao H, Qian K (2013) Shear thickening behavior of nanoparticle suspensions with carbon nanofillers. J Nanopart Res 15:1816. https://doi.org/10.1007/s11051-013-1816-x
35. Gürgen S, Kushan MC, Li W (2016) The effect of carbide particle additives on rheology of shear thickening fluids. Korea Aust Rheol J 28:121–128. https://doi.org/10.1007/s13367-016-0011-x
36. He Q, Gong X, Xuan S, Jiang W, Chen Q (2015) Shear thickening of suspensions of porous silica nanoparticles. J Mater Sci 50:6041–6049. https://doi.org/10.1007/s10853-015-9151-5

37. Gericke M, Trygg J, Fardim P (2013) Functional cellulose beads: preparation, characterization, and applications. Chem Rev 113: 4812–4836. https://doi.org/10.1021/cr300242j
38. Chen LF, Tsao GT (1977) Chemical procedures for enzyme immobilization on porous cellulose beads. Biotechnol Bioeng 19:1463–1473. https://doi.org/10.1002/bit.260191005
39. Gemeiner P, Benes MJ, Stamberg J (1989) Bead cellulose and its use in biochemistry and Biotechnology. Chem Pap 43:805
40. Navarro RR, Sumi K, Fujii N, Matsumura M (1996) Mercury removal from wastewater using porous cellulose carrier modified with polyethyleneimine. Water Res 30:2488–2494. https://doi.org/10.1016/0043-1354(96)00143-1
41. Gonte RR, Balasubramanian K, Mumbrekar JD (2013) Porous and cross-linked cellulose beads for toxic metal ion removal: hg(II) ions. J Polym 2013:1–9. https://doi.org/10.1155/2013/309136
42. Voon LK, Pang SC, Chin SF (2015) Highly porous cellulose beads of controllable sizes derived from regenerated cellulose of printed paper wastes. Mater Lett 164:264–266. https://doi.org/10.1016/j.matlet.2015.10.161
43. Chen KI, Yao Y, Chen HJ, Lo YC, Yu RC, Cheng KC (2016) Hydrolysis of isoflavone in black soy milk using cellulose bead as enzyme immobilizer. J Food Drug Anal 24:788–795. https://doi.org/10.1016/j.jfda.2016.03.007
44. Liu D-M (2000) Particle packing and rheological property of highly-concentrated ceramic suspensions: φm determination and viscosity prediction. J Mater Sci 35:5503–5507. https://doi.org/10.1023/A:1004885432221
45. Kalman DP, Schein JB, Houghton JM et al (2007) Polymer dispersion based shear thickening fluid-fabrics for protective applications. Proc SAMPE 1:3–7
46. Wetzel ED (2004) The effect of rheological parameters on the ballistic properties of shear thickening fluid (STF)-Kevlar composites. AIP Conf Proc 712:288–293. https://doi.org/10.1063/1.1766538
47. Chen Q, Xuan S, Jiang W, Cao S, Gong X (2016) Shear time dependent viscosity of polystyrene-ethylacrylate based shear thickening fluid. Smart Mater Struct 25:45005. https://doi.org/10.1088/0964-1726/25/4/045005
48. Moriana AD, Tian T, Sencadas V, Li W (2016) Comparison of rheological behaviors with fumed silica-based shear thickening fluids. Korea Aust Rheol J 28:197–205. https://doi.org/10.1007/s13367-016-0020-9
49. Huang W, Wu Y, Qiu L, Dong C, Ding J, Li D (2015) Tuning rheological performance of silica concentrated shear thickening fluid by using graphene oxide. Adv Condens Matter Phys 2015:1–5. https://doi.org/10.1155/2015/734250
50. Xu Y, Gong X, Peng C, Sun YQ, Jiang WQ, Zhang Z (2010) Shear thickening fluids based on additives with different concentrations and molecular chain lengths. Chin J Chem Phys 23:342–346. https://doi.org/10.1088/1674-0068/23/03/342-346
51. Lootens D, Hébraud P, Lécolier E, Van Damme H (2004) Gelation, shear-thinning and shear-thickening in cement slurries solid/liquid dispersions in drilling and production fluides chargés en forage et production pétrolière. Oil Gas Sci Technol – Rev IFP 59:31–40
52. Fall A, Bertrand F, Ovarlez G, Bonn D (2012) Shear thickening of cornstarch suspensions. J Rheol (N Y N Y) 56:575–591. https://doi.org/10.1122/1.3696875
53. Boersma WH, Laven J, Stein HN (1992) Viscoelastic properties of concentrated shear-thickening dispersions. J Colloid Interface Sci 149:10–22. https://doi.org/10.1016/0021-9797(92)90385-Y
54. Mewis J, Biebaut G (2001) Shear thickening in steady and superposition flows effect of particle interaction forces. J Rheol (N Y N Y) 45:799–813. https://doi.org/10.1122/1.1359761
55. Gürgen S, Li W, Kushan MC (2016) The rheology of shear thickening fluids with various ceramic particle additives. Mater Des 104: 312–319. https://doi.org/10.1016/j.matdes.2016.05.055
56. Russel WB, Saville DA, Schowalter WR (1989) Colloidal dispersions
57. Macosko CW (1994) Rheology: principles, measurements, and applications. VCH
58. Raghavan S, Khan S (1997) Shear-thickening response of Fumed silica suspensions under steady and oscillatory shear. J Colloid Interface Sci 185:57–67. https://doi.org/10.1006/jcis.1996.4581
59. Wagner NJ, Brady JF (2009) Shear thickening in colloidal dispersions. Phys Today 62:27–32. https://doi.org/10.1063/1.3248476
60. Liang X-H, Guo Y-Q, Gu L-Z, Ding E-Y (1995) Crystalline-amorphous phase transition of poly(ethylene glycol)/cellulose blend. Macromolecules 28:6551–6555. https://doi.org/10.1021/ma00123a023
61. Turhan KN, Sahbaz F, Güner A (2001) A spectrophotometric study of hydrogen bonding in methylcellulose-based edible films plasticized by polyethylene glycol. J Food Sci 66:59–62. https://doi.org/10.1111/j.1365-2621.2001.tb15581.x
62. Kondo T, Sawatari C, Manley RSJ, Gray DG (1994) Characterization of hydrogen bonding in cellulose-synthetic polymer blend systems with regioselectively substituted methylcellulose. Macromolecules 27:210–215. https://doi.org/10.1021/ma00079a031
63. Yang G, Zhang L, Feng H (1999) Role of polyethylene glycol in formation and structure of regenerated cellulose microporous membrane. J Membr Sci 161:31–40. https://doi.org/10.1016/S0376-7388(99)00095-2
64. Zhang GD, Wu JR, Tang LC, Li JY, Lai GQ, Zhong MQ (2014) Rheological behaviors of fumed silica/low molecular weight hydroxyl silicone oil. J Appl Polym Sci 131:8846–8850. https://doi.org/10.1002/app.40722
65. Ye F, Zhu W, Jiang W, Wang Z, Chen Q, Gong X, Xuan S (2013) Influence of surfactants on shear-thickening behavior in concentrated polymer dispersions. J Nanopart Res 15:2122. https://doi.org/10.1007/s11051-013-2122-3